Docking of Cationic Antibiotics to Negatively Charged Pockets in RNA Folds

Thomas Hermann and Eric Westhof*

Institut de Biologie Moléculaire et Cellulaire du CNRS, UPR 9002, 15 rue René Descartes, F-67084 Strasbourg, France

Received October 23, 1998

The binding of aminoglycosides to RNA provides a paradigm system for the analysis of RNA−drug interactions. The electrostatic field around three-dimensional RNA folds creates localized and defined negatively charged regions which are potential docking sites for the cationic ammonium groups of aminoglycosides. To explore in RNA folds the electronegative pockets suitable for aminoglycoside binding, we used calculations of the electrostatic field and Brownian dynamics simulations of cation diffusion. We applied the technique on those RNA molecules experimentally known to bind aminoglycosides, namely, two tobramycin aptamers (Wang, Y.; Rando, R. R. *Chem. Biol.* **1995**, *2*, 281−290): the aminoglycoside-binding region in 16S ribosomal RNA (Moazed, S.; Noller, H. F. *Nature* **1987**, *327*, 389−394) and the TAR RNA from human immunodeficiency virus (Mei, H.-Y.; et al. *Bioorg. Med. Chem. Lett.* **1995**, *5*, 2755−2760). For the aptamers and ribosomal RNA, for which the binding sites of the aminoglycosides are known, a good agreement between negatively charged pockets and the binding positions of the drugs was found. On the basis of variations between neomycin-like and kanamycin-like aminoglycosides in the interaction with the electrostatic field of ribosomal RNA, we propose a model for the different binding specificities of these two classes of drugs. The spatial congruence between the electronegative pockets in RNA folds and binding positions of aminoglycosides was used to dock aminoglycosides to ribosomal and TAR RNAs. Molecular dynamics simulations were used to analyze possible RNA−drug interactions. Aminoglycosides inhibit the binding of the viral Tat protein to TAR RNA; however, the drug-binding sites are still unknown. Thus, our docking approach provides first structural models for TAR−aminoglycoside complexes. The RNA−drug interactions observed in the modeled complexes support the view that the antibiotics might lock TAR in a conformation with low affinity for the Tat protein, explaining the experimentally found aminoglycoside inhibition of the Tat−TAR interaction (Mei, H.-Y.; et al. *Bioorg. Med. Chem. Lett.* **1995**, *5*, 2755−2760).

Introduction

Due to its crucial role in key biological processes of cells as well as of their parasites and viruses, RNA is now acknowledged as a prime target for therapeutic intervention.[4−6] Rational drug design seeks to optimize both binding affinity and selectivity of the compounds under study. Selectivity in drug binding is obtained by targeting specific three-dimensional structural elements of RNA formed by bulges, hairpins, junctions, or asymmetries in the deep and shallow grooves around non-canonical base pairs.[5,7] While shape-sensitive molecular interactions based on van der Waals forces and surface complementarity provide binding selectivity, electrostatic interactions are important for achieving binding strength.[8−12] The great majority of drugs binding to RNA contain positively charged groups which can neutralize the negatively charged backbone phosphates of the RNA. Among these cationic compounds targeted at RNA are benzimidazoles,[13] cyclophanes,[14] diphenylfurans,[15] spermidine−acridine conjugates,[11] and the aminoglycosides[16] (Figure 1a). The latter have been known for a long time as potent antibiotics which bind to specific target sites in the bacterial ribosome.[2,17] Binding of aminoglycosides to the A site of 16S ribosomal RNA (rRNA) can block initiation of translation, elicit premature termination, and cause miscoding ultimately leading to bacterial cell death.[17] The low toxicity of aminoglycosides for higher organisms is due to few mutations present in the eukaryal 16S rRNA which prevent high-affinity binding of the drugs.[18] Other important targets for aminoglycosides are the trans-activating response element (TAR) and the Rev response element (RRE), regulatory RNA motifs of the human immunodeficieny virus (HIV) which are impeded by the drugs in interacting with their cognate viral target proteins Tat and Rev.[3,19,20] Aminoglycosides also act as inhibitors of catalytic RNAs such as the self-splicing group I introns,[21] the hepatitis delta virus ribozymes,[22] and the hammerhead ribozymes of a number of plant viroids.[23]

Experimental and theoretical investigations provide evidence that the high-affinity binding of aminoglycosides to their RNA targets is governed by the electrostatic interactions due to amino groups,[8,10,12,24] positively charged at physiological pH.[25] It has been shown for the hammerhead RNA that upon binding, the aminoglycosides replace Mg^{2+} ions[24] required for both folding and catalysis of the ribozyme.[26,27] However, the mere presence of positive charges in aminoglycosides does not explain how they are able, unlike many other oligocations, to discriminate between different RNA folding motifs. A model has been proposed in which aminoglycosides provide a three-dimensional framework of am-

* Corresponding author. E-mail: Westhof@ibmc.u-strasbg.fr. Fax: + 33-3-88417066. Phone: + 33-3-88417046.

10.1021/jm981108g CCC: $18.00
Published on Web 03/20/1999

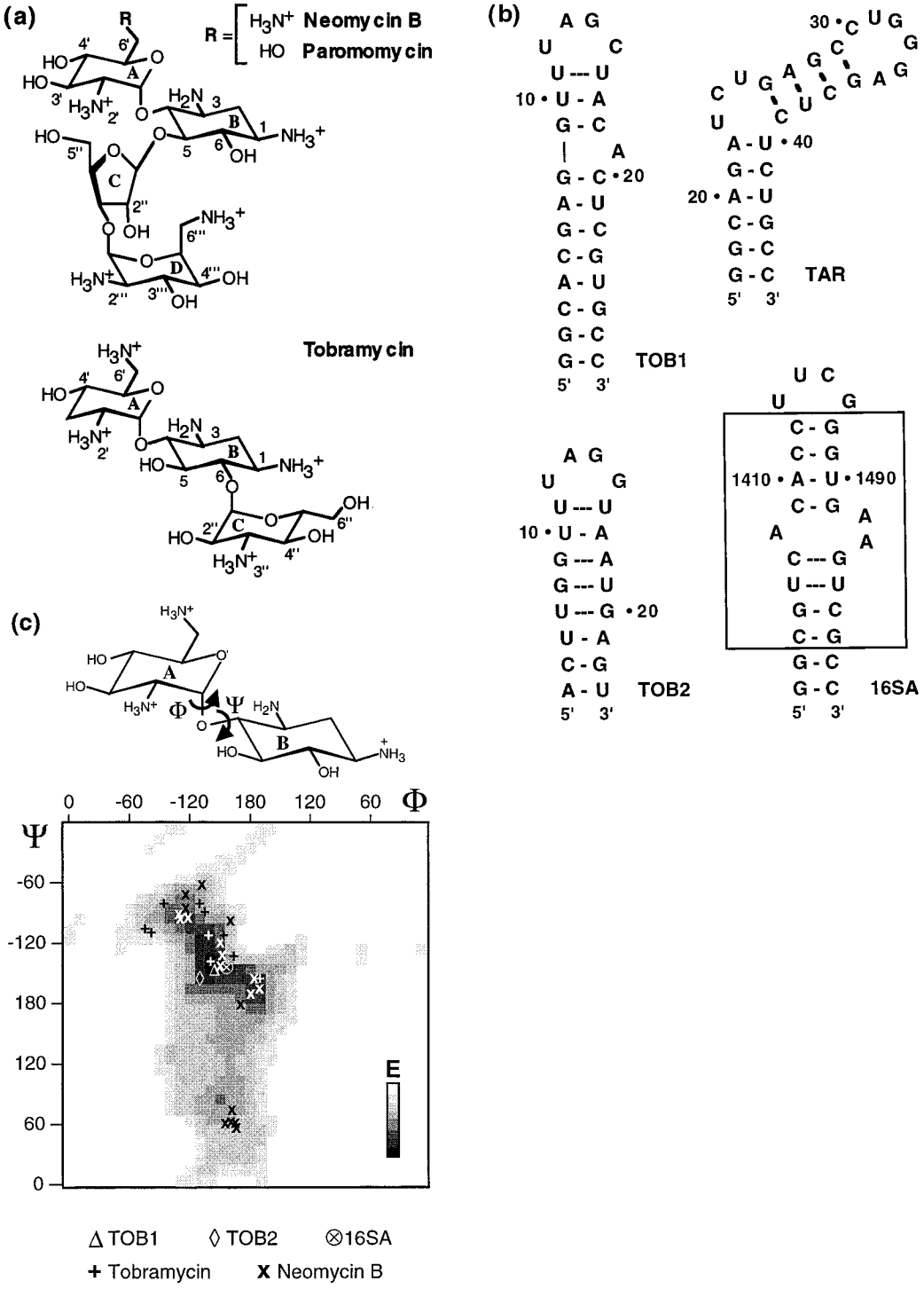

Figure 1. (a) Structures of aminoglycoside antibiotics used in this study. Neomycin B and paromomycin are 4,5-linked 2-deoxystreptamine (2-DOS) derivatives, often referred to as neomycin class aminoglycosides, which comprise four alicyclic rings. Tobramycin belongs to the kanamycin class of 4,6-linked 2-DOS compounds with three rings. The protonation state of amino groups is shown at physiological pH.[25] (b) Secondary structures of RNA molecules for which the interaction with aminoglycosides was investigated. Base pairing is indicated as observed in the three-dimensional structures determined by NMR spectroscopy. Numbering schemes follow the literature. TOB1, TOB2, tobramycin aptamer RNAs;[1,46,47] TAR, HIV-1 TAR RNA;[69] 16SA, oligonucleotide derived from the 16S rRNA A site.[18] In 16SA, the box indicates the nucleotides present in 16S rRNA. (c) Adiabatic map of the two torsion angles connecting rings A and B of the neamine core common in all biologically active aminoglycosides. Indicated on the map are conformations of the neamine moiety in tobramycin complexed with aptamer RNAs (TOB1, TOB2), in paromomycin bound to 16SA, and in solution conformers of free tobramycin (10 conformers) and neomycin (20 conformers) obtained by MD simulations.[10] The map was calculated as described in Methods.

monium groups which can orient in space so as to occupy simultaneously several Mg^{2+} ion-binding sites, thereby displacing cations from their binding pockets in the hammerhead RNA.[10] According to this view, the main basis of target selection of aminoglycosides binding to RNA is structural electrostatic complementarity between the polycationic drugs and the negatively charged three-dimensional fold of the RNA.[10,12]

The hypothesis of electrostatic complementarity can be exploited to propose possible binding sites for aminoglycosides in target RNA molecules. Therefore, it is necessary to know the location of metal ions in the three-dimensional fold of the RNA. Information about metal ion-binding sites in RNA comes from crystal structure analysis[28−34] and biochemical experiments such as metal-induced cleavage[35−38] and interference assays, in which single putative metal-binding phosphate groups in the RNA are substituted with sulfur.[39] While crystal structure analysis provides both the structure of the RNA and the positions of metal ions, it does not exhaustively identify all metal ion-binding pockets as is illustrated by the fact that, for example in tRNAs, more than 10 specific Mg^{2+}-binding sites exist in solution,[40,41] whereas only 3−4 metal ions are found in crystal structures.[42,43] Many three-dimensional structures of RNAs are now solved by NMR techniques, and they do not reveal the positions of metal ions despite the fact that ions are present when the structures are analyzed. We have developed a method to explore negatively charged pockets in RNA three-dimensional folds for which a priori knowledge of metal ion-binding sites is not available.[44] Electronegative pockets may either be considered as metal ion-binding sites or serve as target sites for the docking of positively charged molecule parts such as the ammonium groups of aminoglycosides. The prediction of electronegative pockets is based on the fact that the electrostatic field surrounding a molecule can be calculated from atomic partial charges for a given three-dimensional structure. We use Brownian dynamics (BD) simulations[45] of diffusing positively charged test spheres in order to explore the electrostatic field gradient around RNA molecules.[44] The metal ion-binding sites predicted by BD simulations are then used to dock aminoglycosides to RNA targets, following the hypothesis of electrostatic complementarity.[10]

Here, we test the method on RNA molecules for which the binding sites of aminoglycosides are known from NMR analyses (Figure 1), namely, two aminoglycoside aptamers[1,46,47] and an RNA fragment that contains the aminoglycoside-binding region in the A site of 16S rRNA.[2,18,48−50] On the basis of a discussion of the importance of electrostatic complementarity for the binding of aminoglycosides to RNA targets, we explain the specificity of different drugs. Finally, the novel prediction and docking procedure is applied on the TAR RNA hairpin which is known to bind aminoglycosides[3,20,51,52] but at still unknown locations in the three-dimensional structure.

Results and Discussion

General Outline of the Prediction Method. Negatively charged pockets suitable for cation binding in RNA target molecules are predicted[44] through calculations of the electrostatic field around the three-dimensional folds of the RNAs and Brownian dynamics simulations[45] of cation diffusion.

The prediction was done for three RNA−drug complexes for which the three-dimensional structures had been previously determined,[18,46,47,50] namely, two tobramycin aptamers and an RNA fragment comprising the aminoglycoside-binding region in 16S rRNA (Figure 1). In each case, the BD simulations of cation diffusion were performed on the RNA fold in the absence of the aminoglycoside. The electrostatic complementarity between electronegative pockets of the RNA and positively charged ammonium groups of aminoglycosides was analyzed by comparing the spatial distribution of predicted electronegative regions and the actual positions of ammonium groups in the RNA−antibiotic complexes. The results of the comparisons for the aptamers and the rRNA are described in the following two sections.

In a third section, we demonstrate how the calculation of electronegative pockets can be used to predict the interaction region of positively charged drugs in cases where the three-dimensional structure of an RNA target is known but not the drug-binding sites. The TAR RNA was shown previously to bind aminoglycosides.[3,51,52] Electronegative pockets, predicted for the TAR RNA (Figure 1b), were used for the docking of neomycin B conformers (Figure 1c). Docking was performed by positioning positively charged ammonium groups of solution conformers of the drug into complementary electronegative pockets of TAR. A number of TAR−neomycin complexes with different orientations of the drug were obtained. The possible interactions between the aminoglycoside and the RNA target were then investigated by molecular dynamics (MD) simulations of the modeled TAR−neomycin complexes.

Conformations of Aminoglycosides in Solution and Bound to RNA. Currently, three-dimensional structures are available for three RNA−aminoglycoside complexes which have been investigated by NMR spectroscopy, namely, two tobramycin aptamers[46,47] and the A site of 16S rRNA bound to paromomycin.[18] Interestingly, the conformations of the aminoglycosides in these RNA−drug complexes are similar to the low-energy solution conformations obtained with MD simulations of free solvated aminoglycosides. The conformations of the neamine core in the two aptamer complexes and in the A site complex map to the global minimum on the adiabatic map of the two free torsions in neamine (Figure 1c). The root-mean-square deviation of the two tobramycin conformers found in the aptamer complexes compared to their closest corresponding solution conformations is 0.5 and 1.1 Å, respectively. The similarity between conformations of aminoglycosides free in solution and complexed indicates that RNA recognizes and binds 'native' solution conformers of the drugs without inducing major conformational distortions. This is an important prerequisite validating procedures that use solution conformations of aminoglycosides for docking to RNA targets as will be described below for the TAR RNA.

Tobramycin Aptamers. Aptamer RNAs are oligonucleotides that bind a substrate molecule with both high affinity and specificity.[53] Aptamers for aminoglycoside antibiotics have been obtained from RNA pools of random sequence by in vitro selection (SELEX) using various aminoglycosides as substrates.[1,54−57] The three-dimensional structures of two tobramycin aptamers[1] (TOB1, TOB2) complexed to the aminoglycoside have been recently determined by NMR spectroscopy (Figure

1).[46,47] TOB1 and TOB2 selectively bind tobramycin with an affinity of 9 ± 3 and 12 ± 5 nM, respectively.[1] Tight interaction observed in the complexes between the RNA and the drug suggests that, during the selection process, the RNA evolves into a three-dimensional fold that wraps around the aminoglycoside template to form an optimally specific interaction surface. Thus, it is expected that besides electrostatic interactions, van der Waals contacts may be important for the recognition and binding of tobramycin to the aptamer RNAs.

A. Electronegative Pockets in the Tobramycin Aptamers Explored by BD Simulations. To explore electronegative pockets suitable for binding of positively charged ammonium groups of the aminoglycoside, we performed BD simulations of cation diffusion on the three-dimensional structures of the aptamer RNAs in the absence of the drug. The resulting densities reveal that, in both aptamers, the binding sites for tobramycin superimpose on negatively charged pockets (Figure 2).

In the TOB1 complex, three ammonium groups of tobramycin at positions 2′, 1, and 3" are located close to the center of predicted cation-binding sites of the RNA (Figure 2a). The 6′-ammonium group in the A ring, where the drug was linked to the solid support during RNA aptamer selection,[1] is directed away from the RNA and consequently lies outside the density peaks calculated from BD simulations. The 3-amino group which has the lowest pK_a among all the amino groups on the aminoglycosides[25] also does not dock into an electronegative pocket. This amino group is uncharged at neutral pH values and has probably not been contributing to the electrostatic interaction with the RNA during the selection procedure which was conducted at pH 7.4.[1] Three hydroxyl groups of tobramycin, namely, 5, 2″, and 4″ are pointing with their hydrogens toward predicted cation-binding sites. It could be envisaged that hydroxyl groups can dock into negatively charged pockets, as was suggested for electrostatically restricted water molecules.[44]

While for the TOB1 aptamer complex a good match is observed between the positions of positively charged ammonium groups of tobramycin and discrete electronegative pockets in the RNA, the results for the TOB2 complex are less clear. The density calculated from BD simulations suggests that, compared to TOB1, a less structured electronegative pocket exists within TOB2 where discrete preferred positions for cations are not apparent (Figure 2b). Two of the ammonium groups of tobramycin at positions 1 and 3″ are located within the density, and a third group at 2′ is pointing toward the density peak. These are the same three ammonium groups which interact with electronegative pockets in the TOB1 aptamer. The 3″-ammonium group is pointing toward an extension of the BD densiy peak located below the loop, close to the U7·G20 pair in the stem region of the aptamer. Tobramycin hydroxyl groups 5, 2″, 4″, and 6″ are also located inside the density predicted for TOB2.

B. Comparison of the Two Aptamers. The differences between the electronegative pockets in TOB1 and TOB2 reflect the distinct architectures of the two tobramycin aptamers which, at first sight, are very similar. Both share a common U10−A17 loop segment except at position 15 which is a C in TOB1 and a G in TOB2. In the RNA−drug complexes, the loop segment forms the entrance and walls of the substrate-binding pocket by folding around the aminoglycoside. The loop segment is stacked on a helix with a widened deep groove which constitutes the backside and floor of the binding site. Widening of the RNA deep groove is caused by a bulged nucleotide in TOB1[46] and by three mismatches in TOB2.[47] These distinctive structural motifs lead to characteristic differences between TOB1 and TOB2 in the interaction surface of the aptamers at the backside of the drug-binding pocket (Figure 2c,d, right panels), while the entrance side of the pocket is very similar in both aptamers (Figure 2c,d, left panels). In TOB2, the backside of the pocket is more extensively closed and buried between regions of the RNA backbone causing the electronegative cavity to extend toward the stem region. The accessible surface area of tobramycin ring C (see Figure 1a), penetrating deepest into the binding pocket, is reduced by 98% to 6 Å^2 upon complex formation in TOB2, while the same values for TOB1 are 86% and 36 Å^2, respectively. In total, the reduction of accessible surface area of tobramycin amounts to 74% and 66% when the drug binds to TOB2 and TOB1, respectively. Thus, surface calculations support the findings from BD simulations suggesting that TOB2 forms a deeper tobramycin-binding cavity than TOB1 does. However, the affinity of substrate binding may be more influenced by the depth of the potential inside the electronegative pockets rather than by their spatial extension. TOB1 with its sharply defined cation-binding pockets (Figure 2a) has a higher affinity for tobramycin than TOB2 with its diffuse density (Figure 2b).

16S rRNA A Site. The decoding region of 16S rRNA, which, during translation, provides the site of interaction between the mRNA codon and the aminoacyl-tRNA anticodon, is the primary target for aminoglycoside antibiotics.[2,48] Binding of aminoglycosides to the internal bulge of the A site within the decoding region in bacterial 16S rRNA leads to miscoding during translation. The chemical groups of nucleotides in rRNA required for binding different aminoglycosides have been determined using biophysical and biochemical approaches.[48−50,58−61] The three-dimensional structures of an oligonuclotide analogue representing the A site of 16S rRNA (16SA) (Figure 1b), free in solution and in complex with the neomycin class aminoglycoside paromomycin (Figure 1a), have been recently solved by NMR.[18,62] Although it has been noted that ribosome-free models may be an oversimplification of the situation in vivo,[61] the NMR structure of the 16SA−paromomycin complex provides important insights into the recognition of aminoglycosides by ribosomal RNA.

To study the role of electrostatics for aminoglycoside binding to the rRNA A site, we explored negatively charged pockets in the NMR structures of both the free 16SA and the 16SA−paromomycin complex. We will first describe the calculation of electronegative pockets in free and paromomycin-bound 16SA followed by a discussion of the consequences for aminoglycoside binding. Finally, we will present results from docking aminoglycosides to the negatively charged pockets in the free 16SA.

A. Electronegative Pockets Calculated for Free and Paromomycin-Bound 16S rRNA. BD simula-

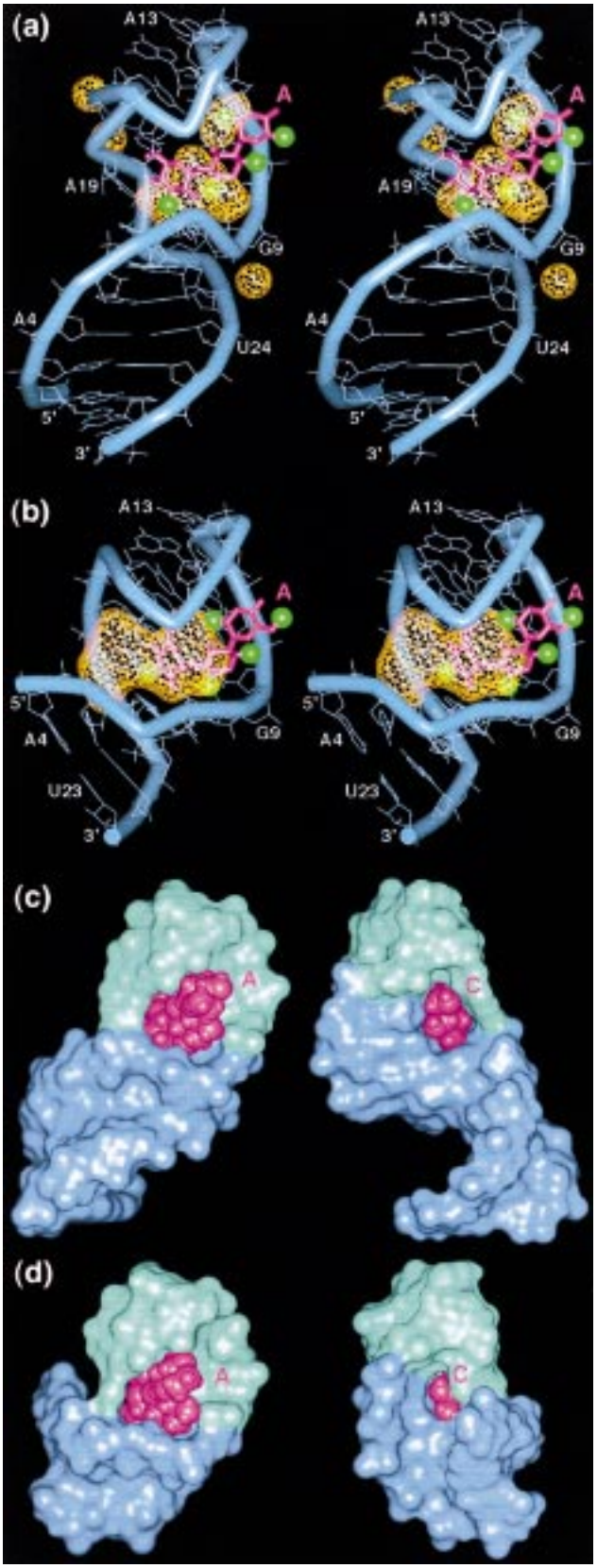

tions of cation diffusion on the free 16SA revealed two discrete rather spherical pockets (1 and 2, Figure 3b) with negative potential within the deep groove of the helically folded bulge structure. The negatively charged pockets are lined by nucleotides of the bulge and the upper and lower stems (Figure 4). The maximum density of pocket 1 is located close to the bases of the U1406·U1495 pair (O4 atoms) and G1494 (O6). For pocket 2, the highest electronegative potential is found at the bases of U1490 (O4) and G1491 (O6).

In contrast to free 16SA, for which two discrete pockets were found, BD simulations predicted a single elongated electronegative cavity within the helically folded bulge structure of the paromomycin-bound 16SA oligonucleotide (Figure 3a). The difference between the shapes of the negatively charged pockets in free and bound 16SA is due to a conformational change induced by the binding of paromomycin to the RNA.[62] Conformational changes are not taken into account by the current method for the calculation of electronegative pockets as the BD simulation of cation diffusion is done with rigid RNA as a target. However, the set of core nucleotides enclosing the cavity in bound 16SA is almost identical with the nucleotides which line the two electronegative pockets in the free conformation (Figure 4). Differences occur at the border of the pocket where C1404 and C1496 are not anymore participating while, in addition, G1489 extends the contact region. The maximum density of the cavity, representing the region where the largest number of diffusing cations was trapped during BD simulations, is located between the phosphates of U1406/C1407 and both phosphates and bases of G1489/U1490. All nucleotides, except for A1492, that are involved in intermolecular contacts to paromomycin in the NMR structure of the 16SA−drug complex[18] participate also in the formation of the electronegative pocket.

However, of the five positively charged ammonium groups in paromomycin (Figure 1a), only the two of ring D (N2‴, N6‴) are found within the calculated density (Figure 3a). The maximum of the electronegative pocket covers the N2‴ ammonium group and is in proximity to the two hydroxyls of ring D (O3‴, O4‴). The hydroxyl groups of ring C are also found within the electronegative density. In contrast, all three ammonium groups of the neamine core (N2′, N1, N3) are located in regions of relatively low electronegative potential formed essentially by the bases on one side of the bulge (G1491−C1496). Thus, only a limited electrostatical complementarity between the electronegative regions of the RNA and positively charged ammonium groups of the aminoglycoside is observed in the NMR structure of the 16SA−paromomycin complex.

The neamine moiety, comprising rings A and B, is not participating in strong electrostatic interactions. Rather, rings A and B are extensively involved in shape-sensitive van der Waals interactions such as stacking

Figure 2. Stereoviews of the aptamer RNAs (blue) TOB1[46] (a) and TOB2[47] (b) complexed with tobramycin (magenta). Cation-binding pockets predicted by BD simulations on the RNAs in the absence of the drug are shown as an orange density grid. The positively charged ammonium groups of tobramycin are indicated by green spheres. During the in vitro selection of both aptamer RNAs, the aminoglycoside was attached to a solid support via its A ring[1] (see Figure 1a) which is the most right of the three rings directed outward into the solvent. The space-filling monoviews (c, d) show the apatmers from the front (left) and the back (right) side of the tobramycin-binding pocket. The U10−A17 loop segment that forms the walls of the substrate pocket in both aptamers is colored in light green. Tobramycin is in magenta.

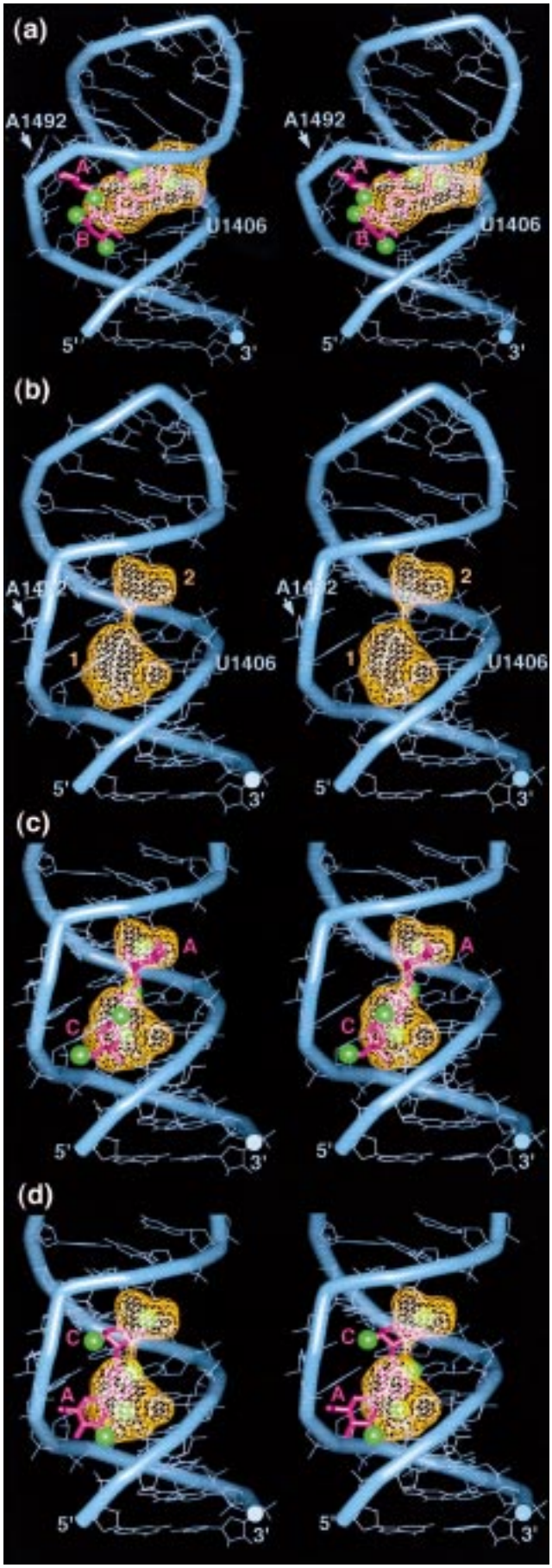

of ring A with the base of G1491. In contrast, rings C and D of paromomycin are located within regions of strong electronegative potential in 16SA. These results of our calculations are in line with experimental findings showing that rings A and B of neomycin class aminoglycosides confer specificity to the binding of antibiotics to 16S rRNA, while rings C and D contribute weakly to the specificity of antibiotic binding and function.[18,50,63] While it has been shown that a certain directionality in the orientation of the positive charge at ring D is necessary for specific binding of neomycin class aminoglycosides to 16S rRNA,[64] this ring is found partially disordered in structures of the 16SA−paromomycin complex determined by NMR spectroscopy.[18] This indicates that the electrostatic interactions between the RNA and positively charged ammonium groups in ring D display a certain plasticity which can accommodate several conformers of the aminoglycoside. Similar observations were made for electrostatic interactions between aminoglycosides and other RNAs, namely, the hammerhead ribozyme[10] and TAR (see below).

B. Differences between Neomycin and Kanamycin Class Antibiotics in the Binding to 16SA. We suggest that the shape-insensitive electrostatic interactions of rings C and D with the negatively charged pocket in 16SA contribute to both the specificity and the strength of neomycin class aminoglycoside binding to the A site oligonucleotide. It was pointed out before that rings C and D of the 4,5-linked 2-DOS derivates (see Figure 1a) might confer a directional specificity to antibiotic binding and ensure a correct interaction of rings A and B with the A site RNA.[50] This directionality in aminoglycoside binding to 16S rRNA may be dependent on the presence of rings C and D binding in the negatively charged cavity. Consequently, one would expect that the directionality is absent for aminoglycosides lacking rings C and D. Indeed, the kanamycin class of aminoglycosides, 4,6-linked 2-DOS compounds comprising three alicyclic rings (see Figure 1a), display lower binding specificity toward 16S rRNA.[61] Unsubstituted neamine, the core moiety of aminoglycosides, binds itself only weakly to 16SA.[50] Data from NMR experiments indicate that alternate conformers of neamine may be sampling multiple binding sites within the deep groove of 16SA[50] similar to aminoglycosides binding to the large electronegative cavity of the hammerhead ribozyme.[10]

The proposed difference in the capability of neomycin and kanamycin class aminoglycosides for binding with a defined directionality to the 16S rRNA A site might have important consequences for the efficiency of these drugs to induce a local conformational change in the

Figure 3. Stereoviews of negatively charged pockets in three-dimensional structures of the 16SA rRNA oligonucleotide. (a) Complex[18] between 16SA (blue) and paromomycin (magenta). The orange density grid marks the electronegative pocket calculated by BD simulations on the RNA in the absence of the drug. Ammonium groups of paromomycin are shown as green spheres. (b) Free 16SA RNA.[62] The two discrete regions of density (orange) calculated by BD simulations are designated 1 and 2, respectively. (c, d) Two representative examples of 16SA−tobramycin complexes obtained by docking of ammonium groups (green) into negatively charged pockets of the free 16SA RNA. Tobramycin is in magenta; ammonium groups are in green.

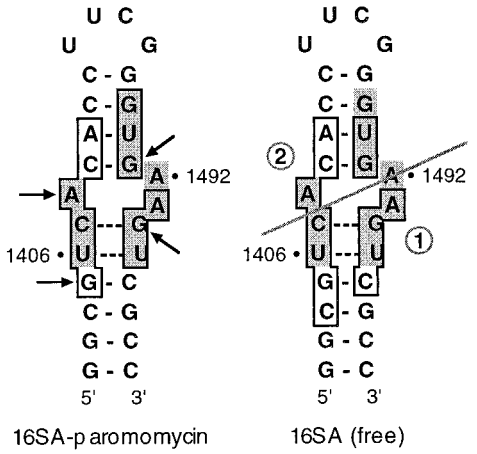

Figure 4. Nucleotides lining the negatively charged pockets in the 16SA oligonucleotide are highlighted with boxes. Residues that form intermolecular contacts with the aminoglycoside in the NMR structure of the 16SA−paromomycin complex[50] are marked on a gray background. Arrows indicate nucleotides that are protected from chemical probes by aminoglycoside antibiotics.[58] The two sets of nucleotides that are bordering the discrete electronegative pockets in 16SA (free) are separated by a gray line and designated 1 and 2, respectively.

RNA (Figure 5). A comparison of the free and paromomycin-complexed conformations of 16SA shows that two bases, A1492 and A1493, are displaced from the deep groove when paromomycin is bound.[62] This local conformational change is accompanied by a slight contraction of the deep groove (see Figure 3a,b). Rings A and B of paromomycin occupy the space where the bases of A1492 and A1493 are located in the free 16SA RNA. The directed positioning of the neamine moiety (rings A and B) in the deep groove might be driven by the electrostatic anchoring of rings C and D in the negatively charged pocket. In contrast to the neomycin-like aminoglycosides, the compounds of the kanamycin class, which comprise three rings and have a more planar shape, may not be able to direct their neamine moiety as to effectively displace A1492 and A1493 from the deep groove. Rather, a number of solution conformers of the drugs might be able to bind in different orientations, among them complexes where the neamine core is inserted into the electronegative cavity (Figure 5). The variable binding modes of kanamycin class aminoglycosides would mainly rely on undirected electrostatic interactions of positively charged ammonium groups, whereas the shape-specific van der Waals contacts outside the negatively charged pocket would be less important as compared to neomycin-like compounds. This might account for the experimentally observed differences between the binding specificities of kanamycin and neomycin class aminoglycosides. Quantitative measurements with surface plasmon resonance on the interaction of aminoglycosides with 16S rRNA have revealed that kanamycin class derivatives, compared to neomycin-like compounds, have affinities lower by at least 2 orders of magnitude and 10-fold lower specificities for binding to 16S rRNA.[61] The lower binding specificity of kanamycin class compounds could be due to several possible binding orientations in the deep groove at the A site of 16S rRNA. Only a few of the binding orientations of the kanamycin-like aminoglycosides might lead to a local conformational change in the RNA by displacing A1492 and A1493. An extreme case is unsubstituted neamine that might form complexes with 16SA in several alternate conformers by exploring various binding sites within the negatively charged cavity. The low biological activity of neamine might result from the fact that it is small enough to bind into the deep groove of 16SA without resulting in a conformational change in the RNA.

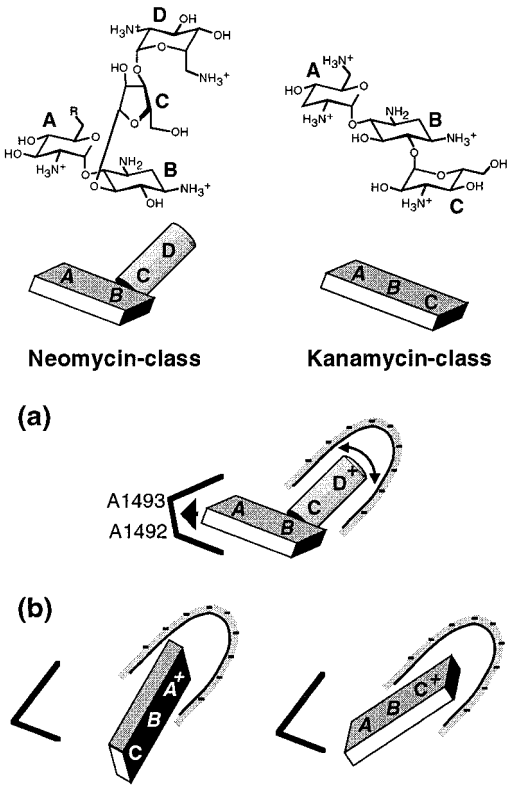

Figure 5. Model for the interaction of 16S rRNA with (a) neomycin class and (b) kanamycin class aminoglycosides. (a) Rings C and D of the 4,5-linked neomycin-like compounds make strong electrostatic contacts in a conformationally flexible manner with an electronegative cavity of 16SA directing the neamine moiety (rings A and B) toward the bases of A1492 and A1493 which are displaced out of the deep groove. (b) The 4,6-linked kanamycin-like aminoglycosides, which are lacking the ring C/D architecture, have a more planar overall shape and may interact in several ways with the electronegative cavity. The neamine moiety of the kanamycin class drugs can, thus, not be anchored in a defined orientation to effectively displace bases in the deep groove of the RNA.

C. Docking of Tobramycin to Free 16SA. To test our assumption that kanamycin-like aminoglycosides could occupy variable binding orientations inside the electronegative cavity of 16SA, we docked solution conformers of tobramycin, a kanamycin-class compound (Figure 1a), to free 16SA. The tobramycin conformers were obtained, as previously described,[10] by high-temperature MD simulations of the free antibiotic in water. Since we were not aiming at an exhaustive survey of RNA−tobramycin interactions, only two low-energy conformers of tobramycin were used for docking, both of which had neamine conformations close to the global energy minimum on the adiabatic map (Figure 1c). The docking was done by positioning ammonium groups of the aminoglycoside into maxima within the electronegative pockets predicted by BD simulations of

cation diffusion. Several different orientations of the tobramycin conformers within the deep groove of 16SA were possible, all displaying a good match between positively charged ammonium groups and negative charge density (Figure 3c,d). In most of the alternative orientations of tobramycin conformers docked to free 16SA, ammonium groups of ring B were positioned in pocket 1 (Figure 4) and pocket 2 was occupied by substituents of either ring A (Figure 3c) or ring C (Figure 3d).

Since both the calculation of electronegative pockets and the docking of aminoglycosides were performed on rigid RNA, there was no way to account for a conformational change as the one occurring when the neomycin class drug paromomycin binds to 16SA.[62] However, the kanamycin-like compound tobramycin fits in various binding orientations into the deep groove of 16SA where the neamine moiety is directed inside the electronegative cavity avoiding sterical clashes with the bases of A1492 and A1493. Thus, binding of kanamycin class aminoglycosides to 16SA might not necessarily induce a conformational change by displacing these bases from the deep groove (Figure 5).

D. Differences between Natural RNAs and Aptamers. The mechanisms of molecular recognition may differ in complexes of artificial aptamer RNAs and natural RNAs such as the 16S rRNA.[6] Aptamers, in contrast to natural RNAs, bind aminoglycosides with both higher affinity and specificity and without competition for metal ions.[1,54,56,65−67] The tobramycin aptamers, for which three-dimensional structures are available (see above), have affinities for structurally related aminoglycosides 10^3-10^4-fold lower than that for tobramycin,[65−67] while the binding constants of natural RNAs such as the 16S rRNA and RRE differ by less than 1 order of magnitude for several different aminoglycosides.[66]

The specific interaction of aminoglycosides with natural targets such as 16S rRNA, HIV TAR, and ribozymes requires the presence of the neamine moiety comprising rings A and B (Figure 1a).[18,50,63] During selection of the tobramycin aptamers, the substrate aminoglycoside was linked via ring A to a solid support, and thus, rings B and C are essentially contributing to the specific interaction between the aminoglycoside and the RNAs. In the artificial aptamer RNAs which wrap around rings B and C of tobramycin, other recognition principles may be favored than those observed in natural RNAs.

HIV-1 TAR RNA. The trans-activating response element (TAR) of HIV and related retroviruses, a hairpin structure at the 5′ end of nascent viral mRNA transcripts (Figure 1), is the binding site for the regulatory Tat protein that increases production of viral mRNAs by enhancing both initiation and processivity of transcribing polymerases in the infected cell.[68] Three-dimensional structures of the free TAR hairpin and Tat−TAR complexes have been determined by NMR revealing a conformational change in the TAR RNA which is induced by binding of the Tat protein into the widened deep groove of the RNA.[69−72] Given its key role in the HIV replication process, the Tat−TAR system is a potential target for anti-HIV therapeutics.[11,73] It has been suggested that small molecules may be able to lock the flexible TAR hairpin structure into a conformation that does not allow for binding of the cognate regulatory protein and, thus, inhibit viral growth.[69] Aminoglycoside antibiotics inhibit the binding of Tat-derived peptides to TAR RNA[3,20] and induce dissociation of preformed Tat−TAR complexes by an allosteric mechanism,[51] with neomycin B (Figure 1a) being the most active compound.

To assess the hypothesis that aminoglycosides may lock TAR in the 'free' conformation observed in the absence of the Tat protein, we searched the three-dimensional structure of the TAR hairpin for cation-binding pockets as potential docking sites for the ammonium groups of aminoglycosides. The investigation proceeded in three steps. First, we analyzed the electrostatic field around the TAR fold by BD simulations of cation diffusion as was described above for the tobramycin aptamers and the 16S rRNA A site. Second, solution conformers of the aminoglycoside neomycin B were docked to TAR by positioning positively charged ammonium groups of the drug into the calculated electronegative pockets of the RNA. Third, we performed MD simulations of the docked TAR−neomycin complexes in order to investigate RNA−drug interactions which could rationalize the inhibition of Tat binding to TAR by aminoglycosides.

A. Electronegative Pockets Calculated for TAR. BD simulations of cation diffusion, performed on the NMR structure of free TAR,[70] revealed three electronegative pockets in the RNA hairpin (Figure 6a). The predicted cation-binding sites are located on top of the U31-GG-G34 loop, in the U23-C-U25 bulge, and in the deep groove of the lower stem. The density peak in the lower stem region is rather extended, involving the backbone of nucleotides in the upper stem which connects the bulge and the loop. Multifunctional drugs, such as the aminoglycosides, carrying several cationic groups could be envisaged to interact simultaneously with the lower and upper stem regions, thereby stabilizing TAR in its free conformation.

B. Docking of Neomycin to TAR. To test the feasibility of this hypothesis, we docked several solution conformers of neomycin B to the TAR RNA. The neomycin conformers (Figure 1c) were obtained, as previously described,[10] by high-temperature MD simulations of the free drug in water. The docking of neomycin to TAR was performed by positioning ammonium groups of the aminoglycoside in discrete maxima within the density grid of cation-binding sites calculated for the RNA. Initially, 20 different solution conformers of neomycin were considered for docking (Figure 1c). Docking ammonium groups into electronegative pockets of the TAR RNA, while avoiding steric clashes, was achieved for 13 neomycin conformers, some of which allowed several different orientations. A total of 27 TAR−neomycin complexes were constructed (Figure 6b,c).

The fact that there is not a single way but several different ways to fit solution conformations of neomycin to electronegative pockets in TAR RNA parallels findings for the hammerhead ribozyme. Solution conformers of aminoglycosides had been docked to crystallographic Mg^{2+} ion-binding sites of the hammerhead RNA yielding

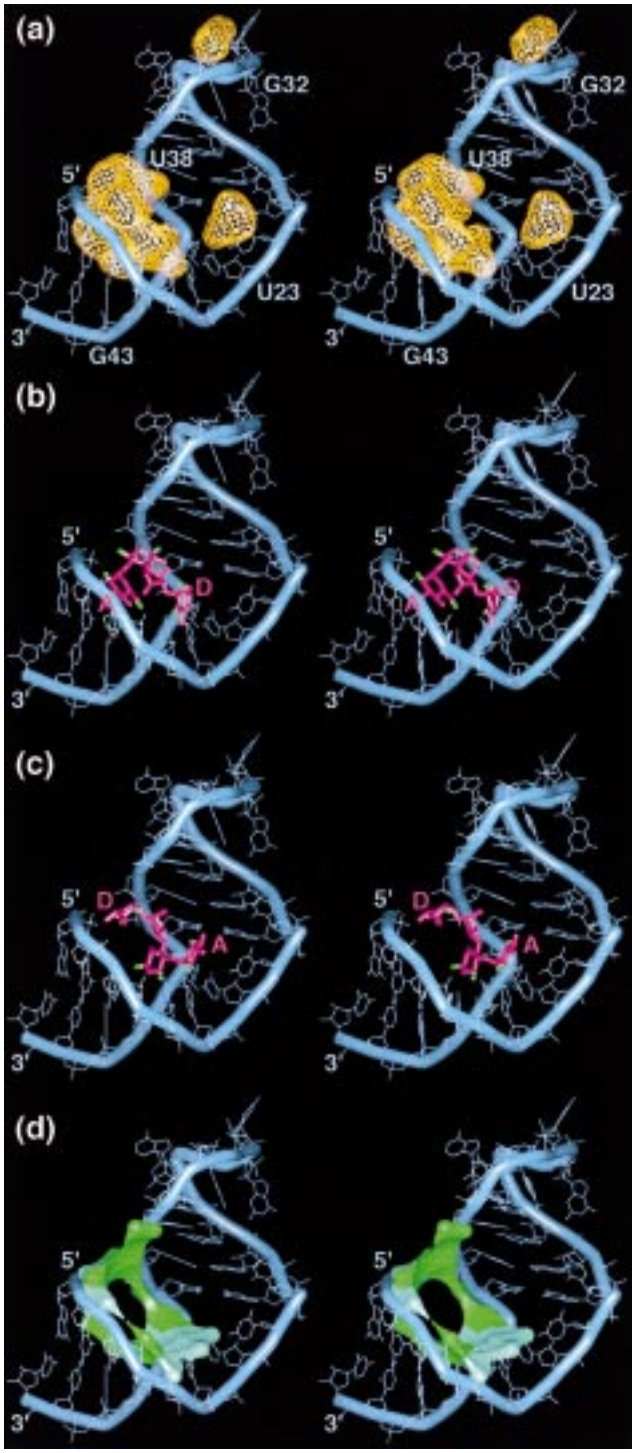

Figure 6. Stereoview of the three-dimensional structure of TAR RNA[70] (blue). (a) Cation-binding pockets predicted by BD simulations (orange density). (b, c) Two representative TAR−neomycin complexes obtained by docking of solution conformers of the drug (magenta) into cation-binding pockets of TAR. Ammonium groups of neomycin are emphasized in green. (d) Summary of recurring interactions between TAR and neomycin B observed in MD simulations of 27 different TAR−neomycin complexes (see also Figure 7). The green surface represents the position of atoms of the RNA that form stable interactions with the drug over the whole simulation period. Light green indicates regions where interactions are observed less frequently than in dark green regions.

16 different complexes for neomycin B.[10] In both natural RNAs, hammerhead ribozyme and TAR, the electrostatic complementarity between the positively charged ammonium groups in aminoglycosides and cation-binding pockets in the RNA folds may provide the basis for high-affinity binding of aminoglycosides. In contrast to artificial aminoglycoside-binding aptamer RNAs that provide a tight pocket for a single conformer, the natural targets for aminoglycosides display more plasticity in accommodating several solution conformers of the drugs inside a high-affinity binding region that is essentially defined by electronegative pockets. This difference is reflected in a lower extent of surface burial of the aminoglycoside in TAR complexes as compared to aptamer complexes. While in the two tobramycin aptamers discussed above at least 66% of accessible surface area of the substrate tobramycin is buried upon complexation, only 50% accessible surface burial is observed for neomycin on the average over the 27 TAR complexes studied here. The promiscuous character of the aminoglycoside-binding sites in natural RNAs may account for the finding that natural RNAs, in contrast to aptamers, bind aminoglycosides with lower affinity and a less discriminatory specificity.[56,65−67]

C. Analysis of TAR−Neomycin Interactions by MD Simulations. General patterns of TAR−aminoglycoside interactions were investigated in MD simulations of the modeled RNA−drug complexes under full solvation conditions. As described previously for hammerhead RNA−aminoglycoside complexes,[10] we performed short MD simulations in which the non-hydrogen atoms of the TAR RNA were fixed at their positions in the NMR structure while the docked neomycin was allowed to move. The MD trajectories calculated for the 27 TAR−neomycin complexes were analyzed for stable hydrogen-bonding patterns in RNA−drug interaction. A compilation of recurring contacts observed during the MD simulations of the complexes is shown in Figure 7. The most important interactions were stable hydrogen bonds between ammonium groups of neomycin and phosphate groups of nucleotides within G18−G21 of the lower stem and C37−C40 of the upper stem (Figure 7a, boxed). Simultaneous interactions of neomycin with these two regions is likely to lock TAR in the 'free' conformation as was suggested above on the basis of the calculated electronegative pockets. Additional contacts, frequently observed in the MD simulations of the TAR−neomycin complexes, are hydrogen bridges to base nitrogen atoms of the G18−G21 stem region and some contacts to uridine O4 atoms (Figure 7a).

In the aminoglycoside, essentially all substituents of the neamine core (rings A and B) were recurrently found involved in hydrogen bonds to the RNA (Figure 7b). Interactions with ring D were fluctuating and strongly dependent on the orientation of neomycin in the particular TAR−drug complex. This is in line with observations in the hammerhead−aminoglycoside system[10] and RRE−aminoglycoside complexes[74] where rings A and B of the drugs provide the most important contacts to the RNA. Rings A and B of the aminoglycosides constitute the neamine moiety (Figure 1c), the invariant unit of most biologically active aminoglycoside antibiotics.

The regions of TAR RNA which were observed to contact neomycin in the MD simulations of the complexes are consistent with results from enzymatic footprinting studies on TAR−neomycin complexes.[51,52] Re-

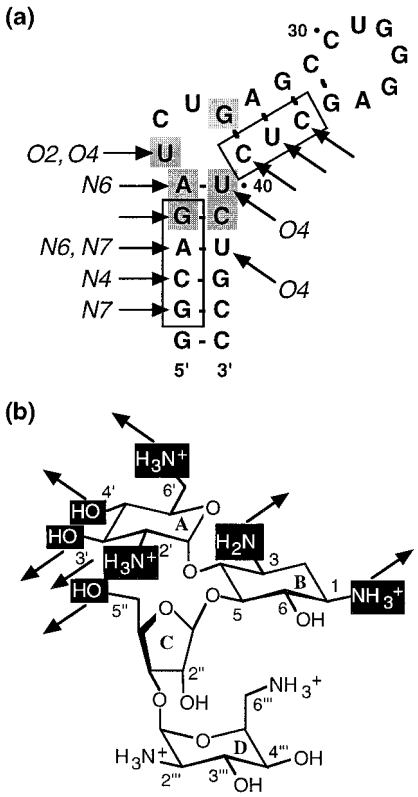

Figure 7. Summary of the interactions between TAR RNA (a) and neomycin B (b) recurrently observed in MD simulations of 27 different TAR−neomycin complexes. (a) In the secondary structure of TAR, nucleotides that engage their phosphate groups in hydrogen bonding to the drug are in outlined boxes. Base atoms involved in interactions with ammonium groups of the drug are given in italic. Essential nucleotides for Tat recognition in the Tat−TAR complex are marked by gray background boxes. (b) Ammonium and hydroxyl groups of neomycin which form hydrogen bonds to the RNA are boxed.

gions protected from hydrolysis by RNases span the lower stem to part of the bulge. However, due to sterical hindrance effects influencing the cleavage of the bulky nucleases, the results from nuclease footprinting give a rather coarse view of the aminoglycoside-binding site. The most significant protection by neomycin has been found at C19.[52]

Interestingly, the phosphate groups of A22, U23, and U40, which have been shown to provide energetically important contacts with the Tat protein,[69,75] are not observed in interactions with neomycin during the MD simulations. Among the other contact sites of Tat in the Tat−TAR complex,[69,76] only the O4 carbonyl oxygen of U23 is involved in hydrogen bonding with neomycin. Thus, the binding of neomycin and the Tat protein involves largely disparate sets of contact sites in TAR RNA. This could account for the observed allosteric mechanism in the aminoglycoside-induced dissociation of preformed Tat−TAR complexes.[51] Aminoglycosides may prevent Tat from binding to TAR not by direct competition for the binding site but by favoring the 'free' conformation of the RNA impeding thereby Tat binding. This hypothesis is consistent with a recent model according to which Tat forms initial contacts with TAR RNA in the widened deep groove and causes a conformational change in the RNA.[77,78]

Conclusions and Perspectives

One important component of the remarkable discriminatory potential of aminoglycosides for selecting RNA targets is the structural electrostatic complementarity between their adaptable three-dimensional framework of positively charged ammonium groups in the antibiotics and the various negatively charged pockets created by the diverse RNA folds. Using Brownian dynamics simulations of cation diffusion, we have explored the electronegative pockets in RNA folds as target regions for the binding of positively charged drugs. The technique has been applied to RNA molecules known to bind aminoglycosides, namely, two tobramycin aptamers: the 16SA oligonucleotide containing the aminoglycoside-binding region in 16S rRNA and the TAR RNA from HIV. In the RNA−aminoglycoside complexes of the aptamers and 16SA, for which the three-dimensional structures are known, the antibiotics are indeed found within negatively charged pockets of the RNAs. On the basis of the complementarity between the electrostatic field created by the RNA fold and the array of positively charged ammonium groups in aminoglycosides, three-dimensional models of TAR−aminoglycoside complexes were deduced and constructed.

Comparing RNA−drug interactions with the contribution of electrostatics in natural and artificial RNAs provides a starting point for manipulating both the binding affinity and the selectivity of aminoglycoside-based compounds.[12] The principle of electrostatic complementarity can be exploited in order to investigate binding sites for positively charged drugs in new RNA targets. In conclusion, the exploration of electronegative pockets in RNA folds by BD simulation provides a powerful new technique for computer-aided drug design.

Methods

Molecular Models and General Procedures. Atomic coordinates of an aptamer RNA−tobramycin complex (TOB1),[46] an oligonucleotide derived from the 16S rRNA A site,[62] a complex thereof with paromomycin,[18] and TAR RNA[70] were extracted from the Brookhaven PDB database. The structure of a second aptamer RNA−tobramycin complex (TOB2)[47] was kindly provided by L. Jiang and D. J. Patel.

Solution conformations of aminoglycosides (Figure 1c) were sampled as previously described by high-temperature MD simulations of the free drugs in water.[10] For neomycin B, used for the docking to TAR RNA, 20 different conformers were obtained which cover the minima on the potential energy surface of the neamine core (Figure 1c). The adiabatic map of unsubstituted neamine was calculated with Insight (Molecular Simulations, San Diego, CA) using CFF91 force-field parameters.[80,81] For tobramycin, 10 different solution conformers were marked on the map. Drawing of molecular surfaces and calculation of surface areas was done with the GRASP program.[81]

Prospection of Negatively Charged Pockets in RNA. Negatively charged pockets in the RNA three-dimensional structures were explored by Brownian dynamics simulations of the diffusion of cationic test spheres in the electrostatic field of the RNAs.[44] Electrostatics was treated with the nonlinear Poisson−Boltzmann equation using a continuum model for the solvent with a dielectric constant of 78 and 4 for water and RNA, respectively. Atomic partial charges for RNA were from the AMBER 4.1 force field.[82]

BD simulations were performed with the UHBD program[45] on rigid RNA targets in the absence of ligands. The diffusing cations were modeled as positively charged spherical probes with radii between 1 and 3.0 Å. A range of radii was used for

the diffusing spheres in order to account for the variation in size of electronegative pockets suitable for either the direct binding or the water-mediated binding of cations and cationic groups.[44] Trajectories of the diffusing test spheres were initiated at randomly chosen points at a distance of 100 Å from the center of mass of the RNA molecule. Trajectories exceeding an outer cutoff sphere of radius 200 Å were terminated. Test spheres that stayed within the cutoff sphere were uniformly simulated for 200 ns at a time step of 0.02 ps. Trajectory coordinates were recorded at intervals of 200 ps. For each probe radius 1000 trajectories were calculated.

For each set of BD trajectories, the probability of finding the center of the charged probe within a discrete volume element in space was calculated as described.[44] The probabilities were visualized as a density grid superimposed on the RNA structure.

Docking of Aminoglycosides to RNA. Rigid body docking of aminoglycoside solution conformers (Figure 1c) to RNA was performed by least-squares fitting of ammonium nitrogen atoms to center-of-mass positions of predicted negatively charged pockets in the RNA structures.[10] Densities obtained in BD simulations of 1 and 1.5 Å test spheres[44] were used throughout to define negatively charged pockets for docking. All possible permutations of correspondences between ammonium groups and predicted pockets were systematically checked for each antibiotic conformer. In each case, conformers were selected that resulted in a fit of ammonium groups into negatively charged pockets, without resulting in sterical clash between the drug and the RNA.

MD Simulations of TAR−Neomycin Complexes. Each RNA−aminoglycoside complex was placed in a rectangular box of SPC/E water containing about 1300 solvent molecules. In all steps of the following calculations the non-hydrogen atoms of the RNA were fixed at their positions in the NMR structure. Initially 1000 steps of conjugate gradient minimization were performed followed by 10 ps of solvent equilibration MD at 298 K with heavy atoms of the aminoglycoside fixed. Subsequently the constraints on the antibiotic were removed, and the system was heated from 10 to 298 K in steps of 50 K over a period of 15 ps; 60 ps of productive MD followed. The MD trajectories were analyzed by time-averaged evaluation of hydrogen bonding between the antibiotic and the RNA.

Acknowledgment. We thank L. Jiang and D. J. Patel (Memorial Sloan-Kettering Cancer Center, New York) for communicating results. T.H. was supported by an EMBO long-term fellowship. E.W. thanks the Institut Universitaire de France for supporting grants.

References

(1) Wang, Y.; Rando, R. R. Specific binding of aminoglycoside antibiotics to RNA. *Chem. Biol.* **1995**, *2*, 281−290.
(2) Moazed, S.; Noller, H. F. Interaction of antibiotics with functional sites in 16S ribosomal RNA. *Nature* **1987**, *327*, 389−394.
(3) Mei, H.-Y.; Galan, A. A.; Halim, N. S.; Mack, D. P.; Moreland, D. W.; Sanders, K. B.; Truong, H. N.; Czarnik, A. W. Inhibition of an HIV-1 Tat-derived peptide binding to TAR RNA by aminoglycoside antibiotics. *Bioorg. Med. Chem. Lett.* **1995**, *5*, 2755−2760.
(4) Pearson, N. D.; Prescott, C. D. RNA as a drug target. *Chem. Biol.* **1997**, *4*, 409−414.
(5) Chow, C. S.; Bogdan, F. M. A structural basis for RNA-ligand interactions. *Chem. Rev.* **1997**, *97*, 1489−1513.
(6) Hermann, T.; Westhof, E. RNA as a drug target: chemical, modelling, and evolutionary tools. *Curr. Opin. Biotechnol.* **1998**, *9*, 66−73.
(7) Burgstaller, P.; Hermann, T.; Huber, C.; Westhof, E.; Famulok, M. Isoalloxazine derivatives promote photocleavage of natural RNAs at G·U base pairs embedded within helices. *Nucleic Acids Res.* **1997**, *25*, 4018−4027.
(8) Wang, H.; Tor, Y. Electrostatic interactions in RNA aminoglycosides binding. *J. Am. Chem. Soc.* **1997**, *119*, 8734−8735.
(9) Li, K.; Fernandez-Saiz, M.; Rigl, C. T.; Kumar, A.; Ragunathan, K. G.; McConnaughie, A. W.; Boykin, D. W.; Schneider, H. J.; Wilson, W. D. Design and analysis of molecular motifs for specific recognition of RNA. *Bioorg. Med. Chem.* **1997**, *5*, 1157−1172
(10) Hermann, T.; Westhof, E. Aminoglycoside binding to the hammerhead ribozyme: a general model for the interaction of cationic antibiotics with RNA. *J. Mol. Biol.* **1998**, *276*, 903−912.
(11) Hamy, F.; Brondani, V.; Flörsheimer, A.; Stark, W.; Blommers, M. J. J.; Klimkait, T. A new class of HIV-1 Tat antagonist acting through Tat-TAR inhibition. *Biochemistry* **1998**, *37*, 5086−5095.
(12) Tor, Y.; Hermann, T.; Westhof, E. Deciphering RNA Recognition: Aminoglycoside binding to the hammerhead ribozyme. *Chem. Biol.* **1998**, *5*, R277−R283.
(13) Wilson, W. D.; Ratmeyer, L.; Zhao, M.; Strekowski, L.; Boykin, D. The search for structure-specific nucleic acid-interactive drugs: effects of compound structure on RNA versus DNA interaction strength. *Biochemistry* **1993**, *32*, 4098−4104.
(14) Fernandez-Saiz, M.; Schneider, H. J.; Sartorius, J.; Wilson, W. D. A cationic cyclophane that forms a base-pair open complex with RNA duplexes. *J. Am. Chem. Soc.* **1996**, *118*, 4739−4745.
(15) Wilson, W. D.; Ratmeyer, L.; Zhao, M.; Ding, D.; McConnaughie, A. W.; Kumar, A.; Boykin, D. W. Design and analysis of RNA structure-specific agents a potential antivirals. *J. Mol. Recog.* **1996**, *9*, 187−196.
(16) Schroeder, R.; von Ahsen, U. Interaction of aminoglycoside antibiotics with RNA. *Nucleic Acids Mol. Biol.* **1996**, *10*, 53−74.
(17) Noller, H. F. Ribosomal RNA and translation. *Annu. Rev. Biochem.* **1991**, *60*, 191−227.
(18) Fourmy, D.; Recht, M. I.; Blanchard, S. C.; Puglisi, J. D. Structure of the A site of *Escherichia coli* 16S ribosomal RNA complexed with an aminoglycoside antibiotic. *Science* **1996**, *274*, 1367−1371.
(19) Zapp, M. L.; Stern, S.; Green, M. R. Small molecules that selectively block RNA binding of HIV-1 Rev protein inhibit Rev function and viral production. *Cell* **1993**, *74*, 969−978.
(20) Mei, H.-Y.; Mack, D. P.; Galan, A. A.; Halim, N. S.; Heldsinger, A.; Loo, J. A.; Moreland, D. W.; Sannes-Lowery, K. A.; Sharmeen, L.; Truong, H. N.; Czarnik, A. W. Discovery of selective small-molecule inhibitors of RNA complexes: the Tat protein/TAR RNA complexes required for HIV-1 transciption. *Bioorg. Med. Chem.* **1997**, *5*, 1173−1184.
(21) von Ahsen, U.; Davies, J.; Schroeder, R. Antibiotic inhibition of group I ribozyme function. *Nature* **1991**, *353*, 368−370.
(22) Rogers, J.; Chang, A. H.; von Ahsen, U.; Schroeder, R.; Davies, J. Inhibition of the self-cleavage reaction of the human hepatitis delta virus ribozyme by antibiotics. *J. Mol. Biol.* **1996**, *259*, 916−925.
(23) Stage, T. K.; Hertel, K. J.; Uhlenbeck, O. C. Inhibition of the hammerhead ribozyme by neomycin. *RNA* **1995**, *1*, 95−101.
(24) Clouet-d'Orval, B.; Stage, T. K.; Uhlenbeck, O. C. Neomycin inhibition of the hammerhead ribozyme involves ionic interactions. *Biochemistry* **1995**, *34*, 11186−11190.
(25) Botto, R. E.; Coxon, B. Nitrogen-15 nuclear magnetic resonance spectroscopy of neomycin B and related aminoglycosides. *J. Am. Chem. Soc.* **1983**, *105*, 1021−1028.
(26) Dahm, S. C.; Uhlenbeck, O. C. Role of divalent metal ions in the hammerhead RNA cleavage reaction. *Biochemistry* **1991**, *30*, 9464−9469.
(27) Long, D. M.; LaRiviere, F. J.; Uhlenbeck, O. C. Divalent metal ions and the internal equilibrium of the hammerhead ribozyme. *Biochemistry* **1995**, *34*, 14435−14440.
(28) Jack, A.; Ladner, J. E.; Rhodes, D.; Brown, R. S.; Klug, A. A crystallographic study of metal-binding to yeast phenylalanine transfer RNA. *J. Mol. Biol.* **1977**, *111*, 315−328.
(29) Pley, H. W.; Flaherty, K. M.; McKay, D. B. Three-dimensional structure of a hammerhead ribozyme. *Nature* **1994**, *372*, 68−74.
(30) Scott, W. G.; Murray, J. B.; Arnold, J. R. P.; Stoddard, B. L.; Klug, A. Capturing the structure of a catalytic RNA intermediate: the hammerhead ribozyme. *Science* **1996**, *274*, 2065−2069.
(31) Cate, J. H.; Doudna, J. A. Metal-binding sites in the major groove of a large ribozyme domain. *Structure* **1996**, *4*, 1221−1229.
(32) Correll, C. C.; Freeborn, B.; Moore, P. B.; Steitz, T. A. Metals, motifs, and recognition in the crystal structure of a 5S rRNA domain. *Cell* **1997**, *91*, 705−712.
(33) Teeter, M. M.; Quigley, G. J.; Rich, A. Metal ions and transfer RNA. In *Nucleic acid-metal ion interactions*; Spiro, T. G., Ed.; Wiley: New York, 1980; pp 145−177.
(34) Pan, T.; Long, D. M.; Uhlenbeck, O. C. Divalent metal ions in RNA folding and catalysis. In *The RNA world*; Gesteland, R. F., Atkins, J. F., Eds.; Cold Spring Harbor Laboratory Press: New York, 1993; pp 271−302.
(35) Brown, R. S.; Hingerty, B. E.; Dewan, J. C.; Klug, A. Pb(II)-catalysed cleavage of the sugar−phosphate backbone of yeast $tRNA^{Phe}$ − implications for lead toxicity and self-splicing RNA. *Nature* **1983**, *303*, 543−546.
(36) Marciniec, T.; Ciesiolka, J.; Wresinski, J.; Krzyzosiak, W. Identification of the magnesium, europium and lead binding sites in *E.coli* and lupine $tRNA^{Phe}$ by specific metal ion-induced cleavages. *FEBS Lett.* **1989**, *243*, 293−298.
(37) Streicher, B.; von Ahsen, U.; Schroeder, R. Lead cleavage sites in the core structure of group I intron-RNA. *Nucleic Acids Res.* **1993**, *21*, 311−317.

(38) Berens, C.; Streicher, B.; Schroeder, R.; Hillen, W. Visualizing metal-ion-binding sites in group I introns by iron(II)-mediated Fenton reactions. *Chem. Biol.* **1998**, *5*, 163−175.
(39) Eckstein, F.; Gish, G. Phosphorothioates in molecular biology. *Trends Biochem. Sci.* **1989**, *14*, 97−100.
(40) Stein, A.; Crothers, D. M. Equilibrium binding of magnesium-(II) by *Escherichia coli* $tRNA^{fMet}$. *Biochemistry* **1976**, *15*, 157−160.
(41) Guéron, M.; Leroy, J. L. Significance and mechanism of divalent-ion binding to transfer RNA. *Biophys. J.* **1982**, *38*, 231−236.
(42) Holbrook, S. R.; Sussman, J. L.; Warrant, R. W.; Church, G. M.; Kim, S. H. RNA-ligand interactions. (I) Magnesium binding sites in yeast $tRNA^{Phe}$. *Nucleic Acids Res.* **1977**, *4*, 2811−2820.
(43) Westhof, E.; Dumas, P.; Moras, D. Restrained refinement of two crystalline forms of yeast aspartic acid and phenylalanine transfer RNA crystals. *Acta Crystallogr. A* **1988**, *44*, 112−123.
(44) Hermann, T.; Westhof, E. Exploration of metal ion binding sites in RNA folds with Brownian dynamics simulations. *Structure* **1998**, *6*, 1303−1314.
(45) Madura, J. D.; Davis, M. E.; Gilson, M. K.; Wade, R. C.; Luty, B. A.; McCammon, J. A. Biological applications of electrostatic calculations and Brownian dynamics simulations. *Rev. Comput. Chem.* **1994**, *5*, 229−267.
(46) Jiang, L.; Suri, A. K.; Fiala, R.; Patel, D. J. Saccharide-RNA recognition in an aminoglycoside antibiotic-RNA aptamer complex. *Chem. Biol.* **1996**, *4*, 35−50.
(47) Jiang, L.; Patel, D. J. Solution structure of the tobramycin-RNA aptamer complex. *Nature Struct. Biol.* **1998**, *5*, 769−774.
(48) Purohit, P.; Stern, S. Interactions of a small RNA with antibiotic and RNA ligands of the 30S subunit. *Nature* **1994**, *370*, 659−662.
(49) Miyaguchi, H.; Narita, H.; Sakamoto, K.; Yokoyama, S. An antibiotic-binding motif of an RNA fragment derived from the A-site-related region of *Escherichia coli* 16S rRNA. *Nucleic Acids Res.* **1996**, *24*, 3700−3706.
(50) Fourmy, D.; Recht, M. I.; Puglisi, J. D. Binding of neomycin-class aminoglycoside antibiotics to the A-site of 16 S rRNA. *J. Mol. Biol.* **1998**, *277*, 347−362.
(51) Wang, S.; Huber, P. W.; Cui, M.; Czarnik, A. W.; Mei, H.-Y. Binding of neomycin to the TAR element of HIV-1 RNA induces dissociation of Tat protein by an allosteric mechanism. *Biochemistry* **1998**, *37*, 5549−5557.
(52) Mei, H.-Y.; Cui, M.; Heldsinger, A.; Lamrow, S. M.; Loo, J. A.; Sannes-Lowery, K. A.; Sharmeen, L.; Czarnik, A. W. Inhibitors of protein-RNA complexation that target RNA: specific recognition of HIV-1 TAR RNA by small organic molecules. *Biochemistry* **1998**, *37*, 14204−14212.
(53) Patel, D. J.; Suri, A. K.; Jiang, F.; Jiang, L.; Fan, P.; Kumar, R. A.; Nonin, S. Structure, recognition and adaptive binding in RNA aptamer complexes. *J. Mol. Biol.* **1997**, *272*, 645−664.
(54) Wallis, M. G.; von Ahsen, U.; Schroeder, R.; Famulok, M. A novel RNA motif for neomycin recognition. *Chem. Biol.* **1995**, *2*, 543−552.
(55) Lato, S. M.; Boles, A. R.; Ellington, A. D. In vitro selection of RNA lectins: using combinatorial chemistry to interpret ribozyme evolution. *Chem. Biol.* **1995**, *2*, 291−303.
(56) Famulok, M.; Hüttenhofer, A. In vitro selection analysis of neomycin binding RNAs with a mutagenized pool of variants of the 16S rRNA decoding region. *Biochemistry* **1996**, *35*, 4265−4270.
(57) Wallace, S. T.; Schroeder, R. In vitro selection and characterization of streptomycin-binding RNAs: recognition discrimination between antibiotics. *RNA* **1998**, *4*, 112−123.
(58) Recht, M. I.; Fourmy, D.; Blanchard, S. C.; Dahlquist, K. D.; Puglisi, J. D. RNA sequence determinants for aminoglycoside binding to an A-site rRNA model oligonucleotide. *J. Mol. Biol.* **1996**, *262*, 421−436.
(59) Spickler, C.; Brunelle, M.-N.; Brakier-Gingras, L. Streptomycin binds to the decoding center of 16 S ribosomal RNA. *J. Mol. Biol.* **1997**, *273*, 586−599.
(60) Blanchard, S. C.; Fourmy, D.; Eason, R. G.; Puglisi, J. D. rRNA chemical groups required for aminoglycoside binding. *Biochemistry* **1998**, *37*, 7716−7724.
(61) Wong, C.-H.; Hendrix, M.; Priestley, E. S.; Greenberg, W. A. Specificity of aminoglycoside antibiotics for the A-site of the decoding region of ribosomal RNA. *Chem. Biol.* **1998**, *5*, 397−406.
(62) Fourmy, D.; Yoshozawa, S.; Puglisi, J. D. Paromomycin binding induces a local conformational change in the A-site of 16 S rRNA. *J. Mol. Biol.* **1998**, *277*, 333−345.
(63) Beneviste, R.; Davies, J. Structure−activity relationships among the aminoglycoside antibiotics: role of hydroxyl and amino groups. *Antimicrob. Agents Chemother.* **1973**, *4*, 402−409.
(64) Alper, P. B.; Hendrix, M.; Sears, P.; Wong, C.-H. Probing the specificity of aminoglycoside ribosomal RNA interactions with designed synthetic analogues. *J. Am. Chem. Soc.* **1998**, *120*, 1965−1978.
(65) Wang, Y.; Kilian, J.; Hamasaki, K.; Rando, R. R. RNA molecules that specifically and stoichiometrically bind aminoglycoside antibiotics with high affinities. *Biochemistry* **1996**, *35*, 12338−12346.
(66) Wang, Y.; Hamasaki, K.; Rando, R. R. Specificity of aminoglycoside binding to RNA constructs derived from the 16S rRNA decoding region and the HIV−RRE activator region. *Biochemistry* **1997**, *36*, 768−779.
(67) Hamasaki, K.; Kilian, J.; Cho, J.; Rando, R. R. Minimal RNA constructs that specifically bind aminoglycoside antibiotics with high affinities. *Biochemistry* **1998**, *37*, 656−663.
(68) Frankel, A. D.; Young, J. A. T. HIV-1: fifteen proteins and an RNA. *Annu. Rev. Biochem.* **1998**, *67*, 1−25.
(69) Aboul-ela, F.; Karn, J.; Varani, G. The structure of the human immunodeficiency virus type-1 TAR RNA reveals principles of RNA recognition by Tat protein. *J. Mol. Biol.* **1995**, *253*, 313−332.
(70) Aboul-ela, F.; Karn, J.; Varani, G. Structure of HIV-1 TAR RNA in the absence of ligands reveals a novel conformation of the trinucleotide bulge. *Nucleic Acids Res.* **1996**, *24*, 3974−3981.
(71) Ye, X.; Kumar, R. A.; Patel, D. J. Molecular recognition in the bovine immunodeficiency virus TAT peptide-TAR RNA complex. *Chem. Biol.* **1995**, *2*, 827−840.
(72) Puglisi, J. D.; Chen, L.; Blanchard, S.; Frankel, A. D. Solution structure of a bovine immunodeficiency virus Tat-TAR peptide-RNA complex. *Science* **1995**, *270*, 1200−1203.
(73) Hamy, F.; Felder, E. R.; Heizmann, G.; Lazdins, J.; Aboul-Ela, F.; Varani, G.; Karn, J.; Klimkait, T. An inhibitor of the Tat/TAR RNA interaction that effectively suppresses HIV-1 replication. *Proc. Natl. Acad. Sci. U.S.A.* **1997**, *94*, 3548−3553.
(74) Leclerc, F.; Cedergren, R. Modeling RNA-ligand interactions: the Rev-binding element RNA-aminoglycoside complex. *J. Med. Chem.* **1998**, *41*, 175−182.
(75) Pritchard, C. E.; Grasby, J. A.; Hamy, F.; Zacharech, A. M.; Singh, M.; Karn, J.; Gait, M. J. Methylphosphonate mapping of phosphate contacts critical for RNA recognition by the human immunodeficiency virus Tat and rev proteins. *Nucleic Acids Res.* **1994,** *22*, 2592−2600.
(76) Hamy, F.; Asseline, V.; Grasby, J.; Iwai, S.; Pritchard, C.; Slim, G.; Butler, P. J. G.; Karn, J.; Gait, M. Hydrogen bonding contacts in the major groove are required for human immunodeficieny virus type-1 Tat protein recognition of TAR RNA. *J. Mol. Biol.* **1993**, *230*, 111−123.
(77) Huq, I.; Rana, T. M. Probing the proximity of the core domain of an HIV-1 Tat fragment in a Tat-TAR complex by affinity cleaving. *Biochemistry* **1997**, *36*, 12592−12599.
(78) Wang, W.; Rana, T. M. RNA-protein interactions in the Tat-trans-activation response element complex determined by site-specific photo-cross-linking. *Biochemistry* **1998**, *37*, 4235−4243.
(79) Dinur, U.; Hagler, A. T. New approaches to empirical force fields. *Rev. Comput. Chem.* **1991**, *2*, 99−164.
(80) Gundertofte, K.; Liljefors, T.; Norrby, P. O. A comparison of conformational energies calculated by several molecular mechanics methods. *J. Comput. Chem.* **1996**, *17*, 429−449.
(81) Nicholls, A.; Sharp, K. A.; Honig, B. Protein folding and association: insights from the interfacial and thermodynamic properties of hydrocarbons. *Proteins* **1991**, *11*, 281−296.
(82) Cornell, W. D.; Cieplak, P.; Bayly, C. I.; Gould, I. R.; Merz, K. M.; Ferguson, D. M.; Spellmeyer, D. C.; Fox, T.; Caldwell, J. W.; Kollman, P. A. A second generation force field for the simulation of proteins, nucleic acids and organic molecules. *J. Am. Chem. Soc.* **1995**, *117*, 5179−5197.

JM981108G